Earth and Planetary Science Letters 525 (2019) 115747

Contents lists available at ScienceDirect

Earth and Planetary Science Letters

www.elsevier.com/locate/epsl

Lead isotopes as tracers of crude oil migration within deep crustal fluid systems

Nadège Fetter [a,b], Janne Blichert-Toft [a,*], John Ludden [b], Aivo Lepland [c], Jorge Sánchez Borque [d], Erica Greenhalgh [b], Bruno Garcia [e], Dianne Edwards [f], Philippe Télouk [a], Francis Albarède [a]

[a] Laboratoire de Géologie de Lyon, Ecole Normale Supérieure de Lyon, CNRS UMR 5276, Université de Lyon, 46 Allée d'Italie, 69007 Lyon, France
[b] The Lyell Centre, British Geological Survey, Heriot Watt University, Research Avenue South, Edinburgh EH14 4AP, UK
[c] Geological Survey of Norway, P.O. Box 6315 Torgarden, 7491 Trondheim, Norway
[d] Norwegian Petroleum Directorate, Professor Olav Hanssens vej 10, 4021 Stavanger, Pb. 600, 4003 Stavanger, Norway
[e] IFP Energies Nouvelles, 1-4 Avenue du Bois Préau, 92500 Rueil-Malmaison, France
[f] Resources Division, Geoscience Australia, Jerrabomberra Ave, Symonston, Canberra ACT 2609, Australia

ARTICLE INFO

Article history:
Received 10 April 2019
Received in revised form 28 July 2019
Accepted 29 July 2019
Available online xxxx
Editor: L. Derry

Keywords:
crude oil
black shales
Pb isotopes
oil migration
Northern Europe
porous-media convection

ABSTRACT

Although Pb, U, and Th may be fractionated between crude oil and formation waters, Pb isotopes are not. This unique property makes Pb isotopes a particularly useful marker of hydrocarbon generation and migration. Here we show that Pb isotopes offer a new vision of long-range (secondary) oil migration relevant to the formation of oil fields. North Sea oils are largely generated from Jurassic black shales, yet their Pb isotopes are mixtures of Cenozoic to Proterozoic end-members. The same observation is made for crude oils from the Paris Basin, the Barents Sea, Libya, Kuwait, Kazakhstan, and Australia. Bulk Pb in crude oil therefore, for the most part, is foreign to its source rock(s). Our high-precision Pb isotope data on 195 crude oils worldwide, the first such data set in the published literature, and 17 Northern European black shales indicate that deep-seated Pb components originating beneath the source rocks are ubiquitous in crude oil. This implies that oil fields are embedded in basinal convective systems of hydrous fluids heated from below. Plumes of hot fluids rise from the lower thermal boundary layer, which Pb isotopes require douse the basement, into the core of the porous-flow convective cell where they dissolve the newly formed hydrocarbons sequestered in the source rocks. The fluids finally unload unmixed formation waters and crude oil at the base of the upper (conductive) boundary layer where they can be trapped in favorable sites. Based on these new insights we argue that Pb isotopes in crude oil constitute a good tracer of oil migration.

1. Introduction

Petroleum formation requires at least two distinct stages: hydrocarbon formation from organic compounds present in the source rock and migration from the source rock into reservoirs. As formulated by Mann (1994), however, '*the precise mechanism of primary petroleum migration has been elusive despite intensive investigation and discussion.*' Organic geochemistry and the stable isotopes of C, S, and O have long been used to study the processes controlling oil genesis and evolution, while inorganic tracers have so far largely failed to demonstrate the same usefulness as in igneous and sedimentary geochemistry (e.g., Prinzhofer et al., 2009). The limited amount of published data on trace elements and radiogenic and heavy metal isotopes in crude oil bear out both the analytical challenge and lack of information and first-order patterns that could improve the understanding of oil generation. Crude oil is notoriously difficult to mineralize and represents a daunting matrix problem for mass spectrometric techniques that require a high degree of element purity. Data on elemental concentrations are known to scatter widely and to be non-reproducible (e.g., Ventura et al., 2015). Water-hydrocarbon unmixing at low temperature (Mączyński et al., 2004) is the most likely cause of the large range observed for metal abundances (e.g., Ventura et al., 2015). Although numbers may vary from one hydrocarbon to the next, typical water solubility in oil is ~20 mol% at about 250 °C and reduces to ~0.1 mol% below 35 °C (Glandt and Chapman, 1995; Griswold and Kasch, 1942). This temperature dependence of water solubility in crude oil creates a major issue in interpreting chem-

* Corresponding author.
E-mail address: jblicher@ens-lyon.fr (J. Blichert-Toft).

https://doi.org/10.1016/j.epsl.2019.115747
0012-821X/

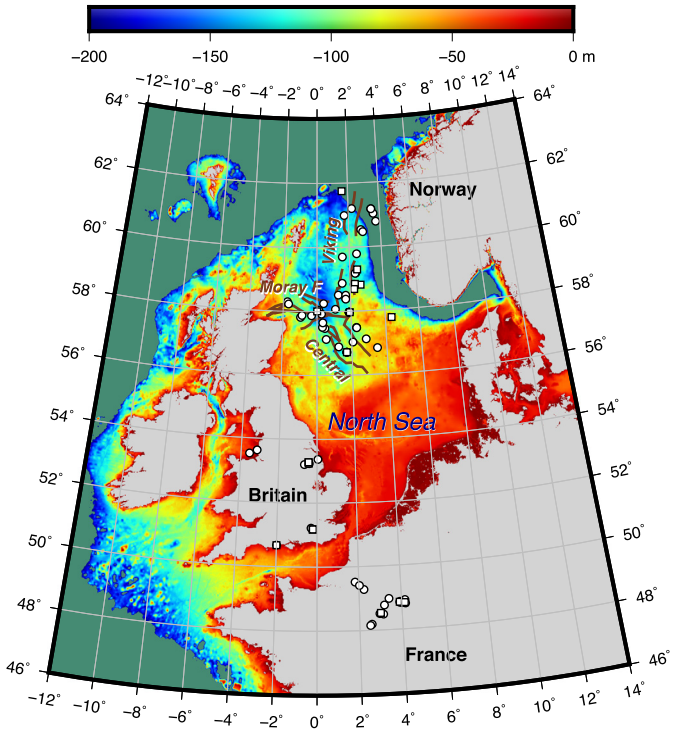

Fig. 1. Map of the North Sea and surrounding regions displaying the locations of 93 crude oils. Depths in excess of 200 m are dark green. Samples with low model Th/U are shown as squares, while the rest of the samples are shown as circles. Major structural features of the North Sea grabens are sketched with brown lines. Six crude oils from the Barents Sea plot off the map (samples 7120/1-3, 7121/7-2, 7122/7-1, 7128/4-1, 7220/11-1, and 7222/6-1 S in Table S1). A similar map for Libya (Fig. 2) is intended to show the correlation between oil finds and volcanic activity. (For interpretation of the colors in the figure(s), the reader is referred to the web version of this article.)

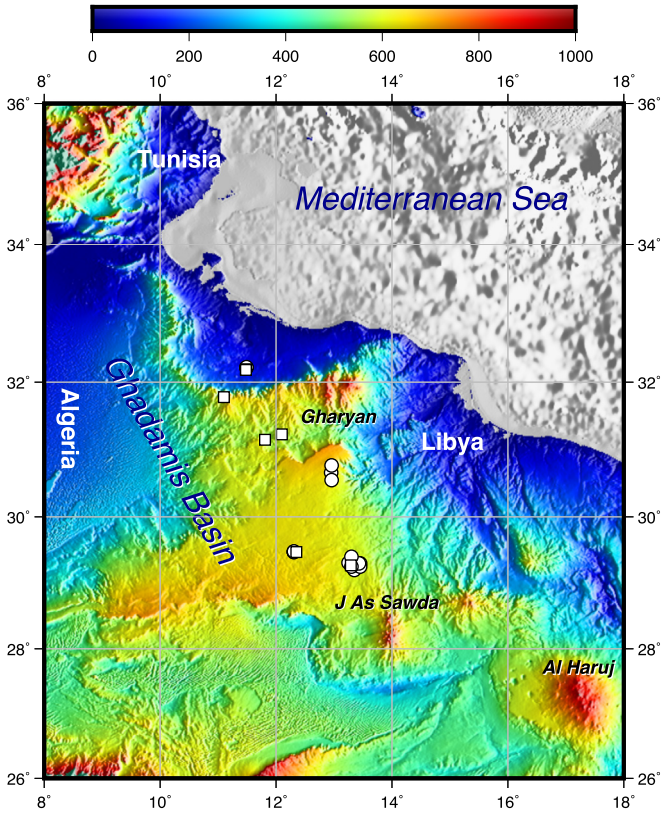

Fig. 2. Map of Northern Libya showing 25 crude oil sites. Samples with low Th/U are displayed as squares, the rest as circles. Names in italic show the volcanic centers of the Neogene Al Haruj province (Elshaafi and Gudmundsson, 2017).

ical and isotopic data obtained on natural hydrocarbons. Water circulates in sedimentary basins by porous flow and through fractures. It is largely exsolved during the adiabatic cooling of crude oil upon emplacement in the thermal boundary layer of the crust (the upper 2-5 km). From this follows that a significant fraction of metals must be lost in the process, in addition to loss during pumping and extraction. Overall, water-oil separation during extraction from the underground therefore rules out most trace elements as markers of oil-related processes, leaving only heavy isotopes, which are not readily fractionated by phase separation, as potentially reliable inorganic tracers. Since uranium is known to correlate positively with organic carbon contents of sediments, in particular carbon-rich black shales (e.g., Leventhal, 1991), exploring Pb isotopes in crude oil as tracers of hydrocarbon generation and migration seems to be a worthwhile avenue for further research. A major advantage of using Pb isotopes over stable isotopes of elements such as C, N, S, V, and Ni is that Pb isotopic variability at the percent level is created by the radioactive decay of ^{238}U, ^{235}U, and ^{232}Th, which contrasts with the thermodynamic isotope effect at a level one to two orders of magnitude smaller. In addition, because Pb isotopic variations are controlled by multiple radioactive systems, their interpretation does not depend on measured parent/daughter ratios. In this respect, Pb isotopes differ from Os isotopes, which cannot be understood without knowledge of the Re/Os ratio, a variable that is subject to fractionation during oil formation and migration (Mahdaoui et al., 2015; DiMarzio et al., 2018). The U-Th-Pb isotope systems, therefore, appear particularly well suited to the study of oil generation and migration.

Further to our work on developing a technique that efficiently extracts Pb and Zn from crude oil for high-precision isotopic analysis (Fetter et al., 2019), we here present Pb isotopic compositions for a large suite of crude oil samples (195) from different oil fields and discoveries around the world, with special emphasis on the North Sea and surrounding regions (Fig. 1). The North Sea oil fields sit at the crossroads of Sveconorwegian (mid-Proterozoic) and Caledonian (mid-Paleozoic) orogens to the north and Hercynian (late-Paleozoic) terranes to the south. The pre-Triassic basement is crisscrossed by networks of grabens created during the Mesozoic as an integral part of the North Atlantic rifting (Ziegler, 1992). The geology of the North Sea oil and gas fields is extremely well documented (Evans et al., 2003). Although reservoir geology is often well characterized prior to and during drilling, unequivocally describing the variety of source rocks and their relative contributions is still a challenge. We therefore aimed at addressing the origin of Pb contained in crude oil and putative source rocks. In particular, as organic-rich black shales produce hydrocarbons upon heating (e.g., Hunt, 1984), we analyzed Pb isotopes in 17 black shales from the Kimmeridge Clay and lateral equivalents and other known source rock formations. In addition to Northern Europe, which we use to establish guidelines for the interpretation of Pb isotopes in crude oil in general, we also collected data from oil fields located in the eastern Ghadamis Basin, which extends across Libya, Tunisia, and Algeria (Fig. 2). In Libya, two unconformities mark the Pan-African and Hercynian orogens and define the basement. The principal source rocks are black shales of Silurian and Late Devonian ages (Hallett and Clark-Lowes, 2016) and the oil field strike follows the direction of the Neogene volcanic field of Al Haruj (Elshaafi and Gudmundsson, 2017). We further collected data from Kuwait, Kazakhstan, and Australia. Lead isotope compositions were also measured in crude oil sampled from different stratigraphic layers in the same well at three North Sea localities. The Pb isotope data for the 195 crude oils and 17 black shales analyzed here are listed in Table S1 along with all their pertinent information. Lead, U, and Th concentrations on a subset (36) of the

195 crude oils and all the black shales also are given in Table S1, while major and trace element concentrations for the 36 sample subset of crude oils are listed in Table S2.

2. Methods

The analytical protocol for high-precision Pb isotopic analysis of crude oil by MC-ICP-MS is described in Fetter et al. (2019). It was designed to extract Pb and Zn from small volumes of crude oil and condensates dissolved in dichloromethane in the presence of dilute HBr, which is known to strongly complex these elements. Given the small targeted sample size (<5 ml), inherent sample heterogeneity, and the lack of reliable concentration data on standard reference materials, the extraction yield cannot be estimated precisely. However, two successive extraction steps systematically recover >95% of the total extractable Pb (Fetter et al., 2019). Isotope fractionation upon extraction is consistent with experimental stable isotope fractionation at ambient temperature (10^{-4} to 10^{-5}) and too small to affect the measured Pb isotopic compositions at the present level of precision (100-200 ppm for 204-based ratios and 50 ppm for 206-based ratios) (Fetter et al., 2019).

For the 36 crude oil samples for which major and trace element concentrations, including U, Th, and Pb, were measured in addition to Pb isotopic compositions, the protocol from Fetter et al. (2019) was slightly modified. After a repeated digestion in distilled concentrated HNO_3 and 30% H_2O_2, the samples were dissolved in 1 ml distilled 0.5 M HNO_3 from which 5% aliquots (50 µl) were taken for elemental concentration analyses. Both the aliquots and the remaining 95% fractions were evaporated to dryness at 110 °C. Anion-exchange column chromatography was used to separate Pb for isotopic analysis on the remaining 95% fractions.

For the black shales, a protocol different from that used for crude oil was followed to allow for elemental analyses of U, Th, and Pb on a 5% aliquot and isotopic analysis of Pb on the remaining 95% of the dissolved sample. The black shale samples first were ground in an agate mortar and approximately 1 g of powder was transferred into a PFA Savillex beaker and weighed. The surface layers were removed by aggressive leaching at high temperature as follows: 4 ml 6 M distilled HCl were added to each sample and the closed beakers left to react for 30 min on a hot plate at 130 °C, then 10 min in an ultrasonic bath, 10 min at 130 °C, 5 min in an ultrasonic bath, and finally 5 min at 130 °C. The acid was pipetted out and the samples rinsed twice in distilled water. The leached sample powder was evaporated to dryness at 110 °C. The samples were then dissolved in a mixture of 3:1:0.5 concentrated double-distilled HF:HNO_3:$HClO_4$. The beakers were left overnight at 130 °C, then dried down, first at 130 °C to get rid of the HF and HNO_3, then at 210 °C to eliminate the $HClO_4$. A last dissolution step consisting of 5 ml 6 M distilled HCl was carried out to bring the samples into complete solution. After leaving the closed beakers for 2-3 h at 130 °C, 5% aliquots (250 µl) were taken for elemental concentration analyses, and both the aliquots and the remaining 95% fractions were evaporated to dryness at 110 °C. Lead was eluted from the remaining 95% fractions by the column chromatography procedure described in Fetter et al. (2019).

All elemental and Pb isotopic analyses were done at the Ecole Normale Supérieure in Lyon. Concentration measurements were done on an Agilent 7500CX Q-ICP-MS (Agilent Technologies Inc.), while Pb isotopic analyses were carried out on either a Neptune Plus HR MC-ICP-MS (Thermo Scientific) or a Nu Plasma HR MC-ICP-MS (Nu Instruments Ltd.). The sample preparation procedures for ICP-MS analyses as well as the instrument settings were the same as those in Fetter et al. (2019). Precision on major and trace element concentrations on the Agilent 7500CX Q-ICP-MS was of the order of 5%. Crude oils duplicated at <4% for Pb concentrations (Fetter et al., 2019), while black shale duplicate measurements showed a variation of 10-20%. Crude oil and black shale duplicates were 3-20% for Th concentrations and 30% maximum for U concentrations. The external reproducibility of the measured Pb isotopic compositions, estimated from repeat measurements of NIST SRM 981, was 100-200 ppm (or 0.01-0.02%) for Pb isotope ratios based on 204 ($^{206}Pb/^{204}Pb$, $^{207}Pb/^{204}Pb$, $^{208}Pb/^{204}Pb$) and 50 ppm (or 0.005%) for $^{207}Pb/^{206}Pb$, $^{208}Pb/^{206}Pb$, and $^{207}Pb/^{208}Pb$. Internal run errors for both standards and unknowns (samples) were smaller than the external reproducibility (Table S1).

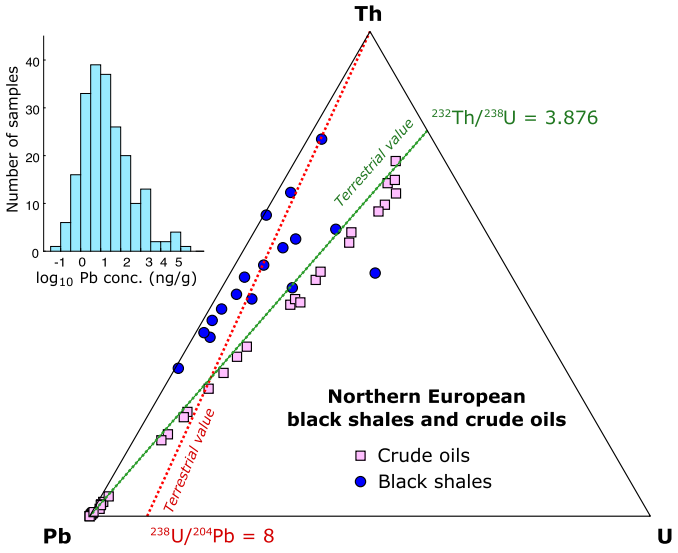

Fig. 3. Ternary plot in Pb-U-Th space showing the U/Pb ($\sim {}^{238}U/^{204}Pb/70 = \mu/70$) and Th/U ($\sim \kappa = {}^{232}Th/^{238}U$) values calculated for 17 black shales and 36 crude oils. Black shales and oil samples are not paired. The green and red dotted lines indicate the terrestrial values of these ratios. Inset: Histogram of Pb concentrations in 195 crude oils.

3. Results

As listed in Table S2, the crude oil samples contain large amounts of Na and K (ranging from a few 100 ppb to >1000 ppm) and, to a lesser extent, Mg, Al, Ca Fe, and Zn (up to several tens of ppm). Lithium, Ti, V, Cr, Mn, Mo, Ni, and Cd abundances vary from one oil sample to the next, with most concentrations being of the order of 0.1-100 ppb, with a few exceptions >1 ppm.

The range of Pb concentrations in the crude oil extracts (Fig. 3, inset; Tables S1 and S2) is very broad (0.1-11,600 ppb, mean = 21 ppb). Given the uncertainties on elemental yields other than that of Pb, we measured U and Th concentrations on only a small subset of crude oil samples (Fig. 3; Tables S1 and S2) but on all the black shales as these were analyzed by bulk dissolution. The $^{238}U/^{204}Pb$ ratios of the crude oil extracts (0.01-142, mean = 27.4) bracket the narrow range of mantle and crust values (7-10), while most of their $^{232}Th/^{238}U$ ratios (1.5-4.1, mean = 3.1) are consistently lower than the planetary value (3.876; Blichert-Toft et al., 2010). The U, Th, and Pb concentration data on the Northern European black shales also are plotted in Fig. 3. In contrast to the oils, all the black shale samples but two have $^{232}Th/^{238}U$ ratios (2.0-142.6, mean = 24.2) significantly higher than the planetary value.

The overall structure of the crude oil Pb isotope data is best understood in 3-dimensional space. Since, due to the noisier signal on the smaller ^{204}Pb peak, ^{204}Pb-normalized ratios are plagued by strong, but misleading, correlations in both 2- and 3-dimensional spaces, we chose to instead represent the overall isotopic variations using ^{206}Pb-normalized ratios. In Fig. 4, the 2-dimensional $^{207}Pb/^{206}Pb$-$^{204}Pb/^{206}Pb$ plot occupies the bottom panel and the $^{208}Pb/^{206}Pb$-$^{204}Pb/^{206}Pb$ plot the back panel.

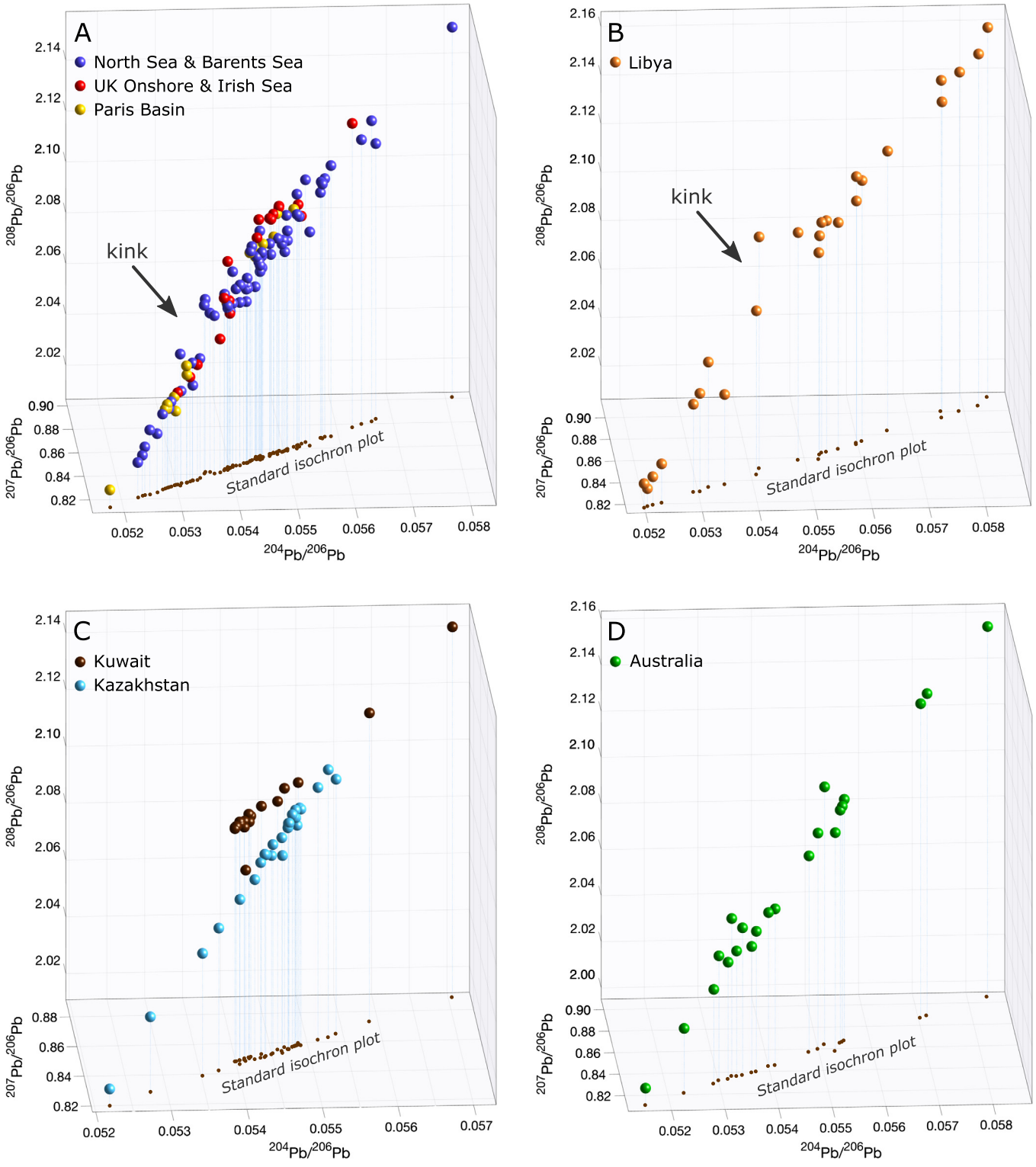

Fig. 4. Three-dimensional representation of Pb isotope compositions for 192 crude oil samples from Northern Europe (top left-hand panel A), Libya (top right-hand panel B), the Middle East (bottom left-hand panel C), and Australia (bottom right-hand panel D). The x-axis ($^{204}Pb/^{206}Pb$) is homologous to the model age calculated from the $^{206}Pb/^{204}Pb$ and $^{207}Pb/^{204}Pb$ ratios (Albarède et al., 2012). The projection onto the bottom panel represents the $^{204}Pb/^{206}Pb$-$^{207}Pb/^{206}Pb$ isochron plot, while the projection onto the back panel represents $^{204}Pb/^{206}Pb$-$^{208}Pb/^{206}Pb$. This 3-dimensional plot shows that Pb from the oil source is accounted for by a mixture of at least three end-members with different ages, U/Pb, and Th/U values.

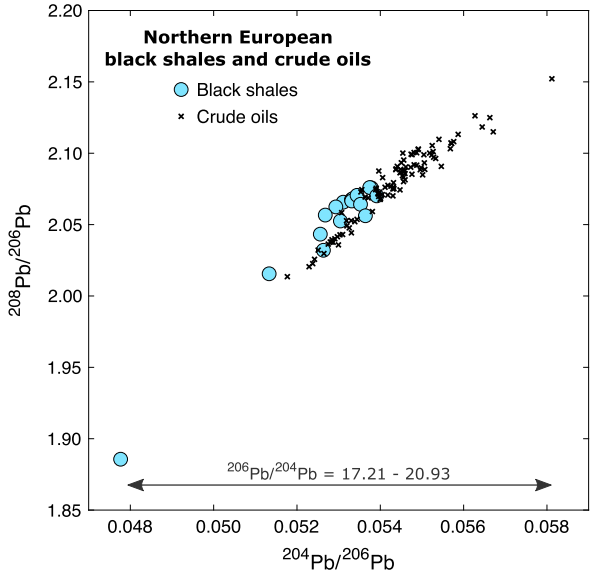

Fig. 5. $^{208}Pb/^{206}Pb$ and $^{204}Pb/^{206}Pb$ of Northern European black shales and North Sea crude oils. The x-coordinate ($^{204}Pb/^{206}Pb$) approximately varies along with the model age, while the intercept of alignments with the y-coordinate ($^{208}Pb/^{206}Pb$) increases with the Th/U ratio. Lead isotopes from most black shales plot as extensions of the crude oil array at its radiogenic (young) end and, therefore, are consistent with these formations, notably the Kimmeridge Clay and its lateral Upper Jurassic stratigraphic equivalents, being the source rocks of the crude oil. Lead nevertheless contains other, much less radiogenic components, which must have been acquired by interaction of connate waters with the basement.

The intercept of a $^{207}Pb/^{206}Pb$ vs $^{204}Pb/^{206}Pb$ array gives the radiogenic (*) $^{207}Pb^*/^{206}Pb^*$ ratio and the model age, while the intercept of a $^{208}Pb/^{206}Pb$ vs $^{204}Pb/^{206}Pb$ array gives the radiogenic $^{208}Pb^*/^{206}Pb^*$ ratio, which itself is proportional to Th/U (or equivalently $\kappa = {}^{232}Th/^{238}U$). If either the age or the Th/U values obtained are geologically inconsistent, the alignments in question represent mixing arrays. The intercepts are listed in Table 1. The $^{207}Pb/^{206}Pb$-$^{204}Pb/^{206}Pb$ alignments of the Northern European oil data and the oil data from the other regions investigated are far too old to represent the age of their source rocks. In addition, the multiplicity of arrays in the corresponding $^{208}Pb/^{206}Pb$-$^{204}Pb/^{206}Pb$ space requires mixing between three sources of Pb or more (Fig. 4). The radiogenic $^{207}Pb^*/^{206}Pb^*$ intercepts defined by the different oil suites, therefore, are not valid chronometers and the ages only 'apparent', not 'true' meaningful geological ages.

The $^{204}Pb/^{206}Pb$-$^{208}Pb/^{206}Pb$ data on Northern European black shales overlap those of oils from the same domain but extend the range towards radiogenic (low $^{204}Pb/^{206}Pb$) Pb (Fig. 5). Black shales may, therefore, be considered end-members of crude oil Pb, but cannot be the only source as they are unable to account for the unradiogenic (high $^{204}Pb/^{206}Pb$) Pb.

The Pb isotope compositions of oils sampled at different depths in the same well are distinct and the ages provided by the intercept of the $^{207}Pb/^{206}Pb$-$^{204}Pb/^{206}Pb$ arrays much older than the permissible migration ages (Tables 1 and S1).

The three-component Pb isotope systematics of oils from the Ghadamis Basin in Libya (Fig. 4B) show similar systematics to those of the North Sea oil fields (Fig. 4A), with unradiogenic Pb consistent with the pre-Pan-African (>540 Ma) basement and a more radiogenic Pb component characteristic of the low-Th/U Phanerozoic sedimentary cover. It is worth noticing that the most unradiogenic samples originate exclusively from prospection provinces NC1 and NC8, situated near the early Paleozoic mounts Nafusah and Qarqaf, respectively (Hallett and Clark-Lowes, 2016). The κ ($^{232}Th/^{238}U$) values derived from the time-integrated $^{208}Pb^*/^{206}Pb^*$ intercepts of all the oil provinces investigated in the present work, excluding Kuwait (with $\kappa \sim 5.69$) but including Australia and Kazakhstan, require that Th/U is significantly lower than the planetary value (Table 1).

4. Discussion

Before exploring the Pb isotope systematics, we first briefly discuss the implications of the concentration data. Except for Th and U, the correlations observed for multiple elements between the logarithms of their concentrations disappear once the concentration data are normalized to the sum of cations, which shows that they reflect a simple dilution effect. We surmise that the solutes analyzed after acid extraction from the 36 crude oil samples could have been trapped either as solid suspensions or as microemulsions of formation water in hydrocarbons (Fetter et al., 2019). In the particular case of Pb and despite the scatter of the data, the high Pb/Al (for a log-normal distribution, average of 0.5 and 1σ range of 0.04-5.2) and Pb/Fe (average of 0.1 and 1σ range of 0.01-1.14) ratios are too high for Pb to be derived from rock fragments. The same observation holds true for Th and U. We therefore conclude that Pb, Th, and U have been introduced into oil by fluids emulsified with the liquid hydrocarbons.

In Pb-Th-U space, black shales and oil fall on opposite sides of the line marking the planetary Th/U value (Fig. 3), which questions the significance of the black shales and raises concerns about elemental fractionation between rock, water, and oil. The lack of more adequate detailed sampling prevents us from determining whether these rocks are an effective source of oil or rather residues after oil expulsion and migration. Circulation of hot hydrous solutions in the sedimentary layers will both increase water solubility in oil and decrease oil viscosity (Glandt and Chapman, 1995), eventually favoring emulsification and oil mobility. Fig. 3 shows that either U depletion of black shales with respect to Pb and Th dates from original sedimentation, as is the case for the few other black shales that have been analyzed from elsewhere (Chen et al., 2009; Jiang et al., 2006), or U was lost at a later stage. In the former case, it would argue for diagenetic remobilization at the time of sedimentation (Anderson and Fleisher, 1991; Barnes and Cochran, 1991), while in the latter case, U was remobilized and preferentially dissolved upon interaction of the black shale protolith with geopressured hydrous fluids at the temperatures of oil generation and migration. Pb-Pb evidence from bitumen (Parnell and Swainbank, 1990) suggests that U may be entrained together with bitumen out of the source rock at the time of hydrocarbon migration but not necessarily by the oil itself. The low U contents of our samples actually require that U was either transported by water migrating with oil or was lost during crude oil extraction.

As for Pb isotopes, they offer a new set of constraints on oil migration. Evidence of mixing inferred from the very old $^{207}Pb^*/^{206}Pb^*$ ages in $^{207}Pb/^{206}Pb$-$^{204}Pb/^{206}Pb$ space (Fig. 4) suggests that oil migration does not lead to complete resetting of the U-Th-Pb isotope systems. The concentration data demonstrate that it is not possible to ignore radiogenic Pb ingrowth after oil formation and two-stage models (Stacey and Kramers, 1975; Albarède et al., 2012) do not strictly apply. It is nevertheless revealing to plot the data in the coordinates of the two-stage model age T_{mod}, μ ($^{238}U/^{204}Pb$), and κ ($^{232}Th/^{238}U \sim$ Th/U) (Fig. S1). Keeping in mind the uncertainties resulting from the ingrowth of radiogenic Pb after oil formation, it is clear that Pb found in Northern European oil samples combine an apparent Mesozoic or younger source, presumably dominated by black shales (Fig. 5), one or more Paleozoic sources, and a Proterozoic source. All of these sources have been previously identified in Pb ores from the same area (Blichert-Toft et al., 2016). Evidence that Pb in oil is a mixture of multiple components, most of them foreign to the source rocks, is reminiscent of the scattered arrays commonly observed in ^{187}Re-^{187}Os isochron

Table 1
Model ages and κ values calculated from, respectively, the intercept of the linear regression in a $^{207}Pb/^{206}Pb$ vs $^{204}Pb/^{206}Pb$ plot, and the intercept in a $^{208}Pb/^{206}Pb$ vs $^{204}Pb/^{206}Pb$ plot, for the black shales and crude oil samples of each region featuring in this study. When several samples in a given region clearly separated into low- and high-Th/U groups, a linear regression was calculated for both sets of values.

Province	$^{207}Pb/^{206}Pb$ vs $^{204}Pb/^{206}Pb$		$^{208}Pb/^{206}Pb$ vs $^{204}Pb/^{206}Pb$	
	Intercept	Inferred age (Ma)	Intercept	Inferred kappa
Black shales				
UK	0.0589 ± 0.0003	561.7 ± 0.1	0.422 ± 0.001	1.689 ± 0.003
Crude oils				
Norway Barents Sea	0.0872 ± 0.0011	1364.3 ± 0.2	0.611 ± 0.002	2.446 ± 0.009
Norway North Sea (low Th/U)	0.0883 ± 0.0771	1387.8 ± 12.2	0.548 ± 0.140	2.192 ± 0.560
Norway North Sea (high Th/U)	0.1039 ± 0.0215	1693.6 ± 2.8	0.939 ± 0.031	3.755 ± 0.123
UK North Sea (low Th/U)	0.0938 ± 0.1341	1502.8 ± 19.6	0.874 ± 0.212	3.495 ± 0.848
UK North Sea (high Th/U)	0.1171 ± 0.0090	1911.7 ± 1.0	1.130 ± 0.010	4.519 ± 0.039
UK Onshore	0.0872 ± 0.0150	1364.7 ± 2.4	0.529 ± 0.031	2.116 ± 0.125
Paris Basin	0.0709 ± 0.0250	954.0 ± 5.2	0.738 ± 0.031	2.952 ± 0.125
Libya (low Th/U)	0.1174 ± 0.0431	1916.4 ± 4.8	0.815 ± 0.059	3.258 ± 0.236
Libya (high Th/U)	0.0710 ± 0.0126	957.1 ± 2.6	1.086 ± 0.015	4.342 ± 0.062
Kuwait	0.1339 ± 0.0412	2148.8 ± 3.9	1.423 ± 0.033	5.692 ± 0.131
Kazakhstan	0.0835 ± 0.0174	1279.1 ± 2.9	0.591 ± 0.033	2.362 ± 0.130
Australia	0.0880 ± 0.0004	1380.7 ± 0.1	0.896 ± 0.001	3.583 ± 0.003

plots (Selby and Creaser, 2005; Finlay et al., 2011; Georgiev et al., 2016). But the consensus is that Re and Os originate in source rocks and massively fractionate into oil, which makes the uptake mechanisms very different from those controlling Pb. The role of coexisting asphaltene and maltene fractions in preserving Pb isotope heterogeneities, as observed by DiMarzio et al. (2018) for Os isotopes, would nevertheless benefit from some clarification.

Overall, the isotopic arrays of Northern European oils and black shales are consistent with them being mixing lines between the three, or more, sources identified above, with variable proportions of each source contributing to the mixtures. Mixing further is confirmed by the ages obtained on different subsets of oil (Table 1). The $^{207}Pb/^{206}Pb$-$^{204}Pb/^{206}Pb$ isochron ages vary from 954 ± 5 Ma to 2149 ± 4 Ma and hence are difficult to explain within a geological context dominated by Paleozoic and Mesozoic tectonic events. Mixing is also confirmed by the kinked $^{208}Pb/^{206}Pb$-$^{204}Pb/^{206}Pb$ arrays (Fig. 4). The apparent κ ($^{232}Th/^{238}U$) of the samples with $^{204}Pb/^{206}Pb$ falling in the range of 0.054-0.056, and therefore associated with Paleozoic events, reaches distinctly lower values than samples associated with both Proterozoic (>0.057) and Cenozoic (<0.054) events (Fig. 4 and S1). The low-κ group is located near the late Jurassic triple junction of the Viking, Moray Firth, and Central grabens (Zanella and Coward, 2003) (Fig. 1). A similar Th/U dichotomy can be observed in Australia and the Ghadamis Basin (Libya) for which the $^{208}Pb/^{206}Pb$-$^{204}Pb/^{206}Pb$ arrays can be accounted for by three distinct Pb components (Proterozoic, Paleozoic, and Cenozoic Pb). All of these observations are consistent with the above discussion of preferential U removal by fluids associated with oil formation.

Lead isotope results suggest that the porous-media convection of hot fluids released by formations underlying the source rocks is a prevalent phenomenon. Osmium isotopes evidence that, in the North Sea, mantle fluids interacted with oil (Finlay et al., 2010). The current paradigm of hydrocarbon expulsion (primary) and long-distance (secondary) migration has been reviewed multiple times (e.g., Tissot and Welte, 1984; Walters, 2017). It appeals to pressure gradients induced by subsidence, compaction, and tectonic liberation (England et al., 1987; Mackenzie et al., 1988), and to the volume expansion resulting from the transformation of kerogen to oil and gas. None of these concepts are intrinsically sufficient to account for the ubiquity of Paleozoic and Proterozoic Pb components in oil.

We will instead try to explain Pb isotope evidence by the temperature-dependent solubility of hydrocarbons in water. The convective porous-flow system of a sedimentary basin should comprise a basal boundary layer, which is the primary source of the hot fluids, a thick, near-adiabatic core ($\partial T/\partial z \sim 0$), and a near-surface conductive boundary layer ($\partial T/\partial z \sim$30-60 °C km^{-1}) (Elder, 1967) (Fig. 6). It is difficult to constrain the depth of the bottom boundary layer, except that the presence of unradiogenic Pb requires that the bottom of the convective system must reach into the basement-sediment interface. Fluid inclusions in source rocks indicate that oil separation from connate waters takes place at temperatures of 100-150 °C (Sverjensky, 1984) near the base of the upper boundary layer, typically at depths of 2-5 km. In sedimentary basins strongly heated from below, plumes of hot fluids, or thermals, rise from the lower boundary layer with particularly strong gradients developing at their front (Graham and Steen, 1994). Although hydrocarbons form from kerogen within a narrow range of temperatures, typically 60-150 °C, experimental evidence shows that they remain stable up to temperatures in ex-

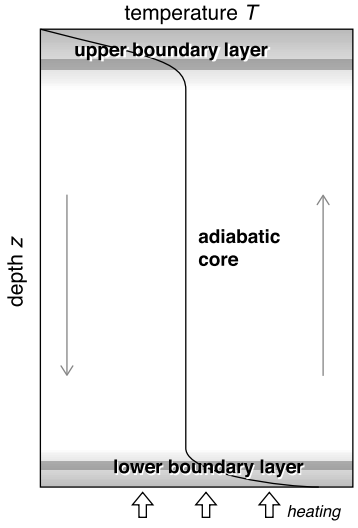

Fig. 6. Temperature distribution in a porous system heated from below (e.g., by a mantle plume). In the core of the system, advective heat transport dominates and temperature distribution is nearly adiabatic ($\partial T/\partial z \sim 0$). Next to the upper and lower boundaries, advective fluid transport drops and conduction becomes the dominant mode of heat transfer. The bottom boundary layer contains excess heat which creates buoyancy and triggers the formation of hot plumes. Old Pb present in oil demands that the bottom boundary layer reaches into the basement. In the upper boundary layer, the temperature distribution is determined by the local geothermal gradient. Hot fluids entering the upper boundary layer cool down very efficiently, which leads to oil–water exsolution.

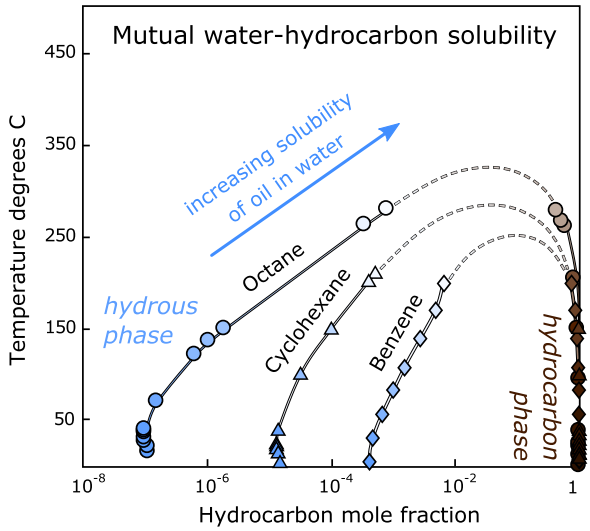

Fig. 7. Mutual solubility of water and octane (Mączyński et al., 2004), one of the abundant hydrocarbons in crude oil, at ambient pressure, cyclohexane (Mączyński et al., 2004), and benzene (Góral et al., 2004). Data above 300 °C are lacking and hence the miscibility loop cannot be closed precisely. Although oil formed in the oil formation window (90-180 °C) and was trapped in the cold thermal boundary layer at around 100 °C, it may nevertheless have been transported without major damage by significantly hotter solutions rising from below the source rocks.

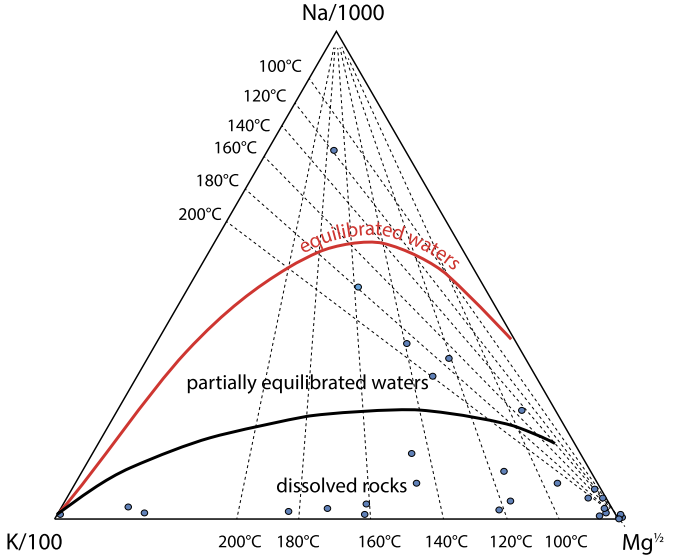

Fig. 8. Ternary plot K-100-Na/1000-Mg1/2 in ppb representing the K-Na and K-Mg thermometers (Giggenbach, 1988). The assumption made here is that water and its solutes were trapped in oil as micro-emulsions and eventually dissolved into oil, and that their present relative abundances in acid extracts (blue dots) reflect those of the trapped waters. K-Na-Mg concentrations seem to initially reflect the composition of the wall-rock (low Na) but, as temperature decreases, become saturated in albite, K-feldspar, and chlorite. Equilibration between water and sequestered oil was never fully achieved but temperatures of 100-180 °C, likely representing the conditions of secondary oil migration and entrapment, are consistent with fluid inclusion evidence (e.g., Sverjensky, 1984).

cess of 250 °C (see references in Mączyński et al., 2004) (Fig. 7). They are therefore readily soluble in hydrous fluids hotter than 150 °C, which facilitates their migration over long distances. At these transport temperatures, the oil solubility contrast between the main body of convective hydrous fluids and the subsurface boundary layer may reach two orders of magnitude. Loading large quantities of liquid hydrocarbons from the source rock therefore requires large-scale percolation of hot fluids in the sedimentary basin. We also investigated whether extract compositions could be used for thermometry by using the Na, K, and Mg abundances determined on the extracts of the oil subset of 36 samples for which we have more complete analyses (Table S2). The data were plotted in Giggenbach's (1988) ternary diagram K/100–Na/1000–$Mg^{1/2}$ (Fig. 8) and apparent equilibration temperatures assessed from the Na-K and K-Mg thermometers. Most samples plot in the field of dissolved rocks (low Na), but the high-Na samples reflect approach to equilibration with feldspar and chlorites and temperatures of 100-180 °C consistent with the conditions of the conductive thermal boundary layer.

Since both water and oil are liquid phases, the predominant factor controlling mutual water-hydrocarbon solubility is temperature, not pressure. The fraction x_{oil} of oil in water typically decreases by an order of magnitude from 150 °C to 50 °C (Mączyński et al., 2004) (Fig. 7) with alkanes being more insoluble than aromatics. At depth z and temperature T, x_{oil} changes according to

$$\frac{\partial \ln x_{oil}}{\partial z} = \frac{\partial \ln x_{oil}}{\partial (1/T)} \times \frac{\partial (1/T)}{\partial z} \approx \frac{\Delta h_{sol}}{RT^2} \times \frac{\partial T}{\partial z}$$

where R is the gas constant and Δh_{sol} the heat of solution of hydrocarbons in water. The solubility effect has been explored by Price (1976), reviewed by Tissot and Welte (1984), and eventually considered inefficient for short-distance (primary) migration. Large temperature gradients, and therefore little differential solubility, are actually not expected at depth in the sedimentary basin and therefore local transport and deposition (primary migration) is unlikely. The conclusion may be different for secondary migration. When taking into account the large differences in mutual solubility of water and oil between deep sedimentary layers and an overlying thermal boundary layer, dissolution of hydrocarbons present in the source rock and exsolution and storage of the resulting oil in shallower reservoirs can be achieved on a regional scale. This is independent of the petrophysical properties of the environment and hot hydrous solutions may be either heated by an underlying magmatic hotspot or remobilized from greater depths and percolating through the Paleozoic and Proterozoic basement (Fig. 9).

Such situations should be common above mantle thermal anomalies, typically magmatic provinces, such as that in Libya (Fig. 2), and tectonic grabens associated with magmatic provinces, such as those in the North Sea (Fig. 1). Additionally, steep thermal gradients also are associated with regional unloading in tectonic foreland basins, such as in Australia where there are no real hotspots.

5. Conclusions

Our high-precision Pb isotope data on 195 crude oils worldwide, the first such data set in the published literature, and 17 Northern European black shales, as well as U, Th, and Pb concentration data on 36 of the crude oils and all 17 black shales, shed new light on oil migration processes. The Pb isotope data require that Pb in crude oils systematically is a mixture of components of different ages ranging from Cenozoic to Proterozoic, and that ingrowth of radiogenic ^{206}Pb, ^{207}Pb, and ^{208}Pb is significant since the parent-daughter ratios U/Pb and Th/Pb of the analyzed oils are much higher than anticipated. This raises the question as to the origin of early Paleozoic and late Proterozoic Pb in hydrocarbons derived from black shales of early Paleozoic to Mesozoic geological age. We suggest a model of oil migration in which deep-seated hot basinal waters derived from the underlying basement and thus carrying a more unradiogenic Pb isotopic signature than that of the source rocks, dissolve hydrocarbons sequestered within the source rocks and along their migration paths and redistribute these into the cooler shallower tectonic traps of the upper thermal boundary layer. Such a process bears consideration by those working in oil genesis as the data presented here highlights the importance of

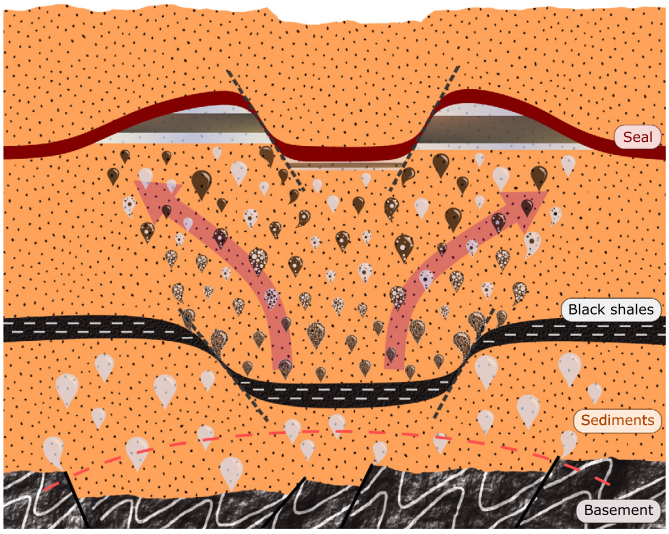

Fig. 9. Cartoon of oil field genesis. Water containing Pb, including Paleozoic and Proterozoic components, i.e., much older than the lower Paleozoic or Mesozoic source rocks, percolates through the basement (bottom dark grey layer with folding pattern) and rises by porous flow through the overlying sedimentary basin, presumably at the top of a deep thermal source. The red dashed line represents such an undefined isotherm. Water is represented as light grey drops. Hot waters dissolve organic material as they pass through carbon-rich black shales (black layer with white dashed lines), possibly along faults (dark grey dashed lines). Water unloads its hydrocarbon component (black drops) as the fluids migrate laterally and upwards through porous sedimentary layers (purple arrows) and oil solubility in water drops exponentially with temperature. Both water and oil get trapped as separate phases below a sealing layer (shown in red).

an underestimated role of mutual oil-water solubility which allows long-distance (secondary) migration of hydrocarbons. This interpretation of the present Pb isotope data shows that oil fields are embedded in large-scale basin-wide fluxes of deep-seated hot fluids.

Acknowledgements

We thank two anonymous referees and the Editor, Lou Derry, for constructive and insightful reviews. We further thank Gareth Harriman from GHGeochem, Lundin Norway AS, the Norwegian Petroleum Directorate, IFP Energies Nouvelles, and Geoscience Australia, the latter through Andrew Owen, for providing the crude oil samples analyzed in this study. The British Geological Survey (BGS) via Tracey Gallagher is thanked for providing the black shales and Olivier Donard for providing the NIST 1634c standard reference material. The British Geological Survey (NERC-UKRI) further provided funding for the analytical work to JB-T and NF as part of the BGS Universities Funding Initiative (BUFI). We are grateful to Florent Arnaud-Godet for help with clean laboratory maintenance, acid distillation, and occasional instrument assistance.

Appendix A. Supplementary material

Supplementary material related to this article can be found online at https://doi.org/10.1016/j.epsl.2019.115747.

References

Albarède, F., Desaulty, A.-M., Blichert-Toft, J., 2012. A geological perspective on the use of Pb isotopes in archaeometry. Archaeometry 54, 853–867.
Anderson, R.F., Fleisher, M.Q., 1991. Uranium precipitation in Black Sea sediments. In: İzdar, E., Murray, J.W. (Eds.), Black Sea Oceanography. In: NATO ASI Series (Series C: Mathematical and Physical Sciences), vol. 351. Springer.
Barnes, C.E., Cochran, J.K., 1991. Geochemistry of uranium in Black Sea sediments. Deep-Sea Res., A, Oceanogr. Res. Pap. 38 (suppl. 2), S1237–S1254.
Blichert-Toft, J., Zanda, B., Ebel, D.S., Albarède, F., 2010. The Solar System primordial lead. Earth Planet. Sci. Lett. 300, 152–163.
Blichert-Toft, J., Delile, H., Lee, C.-T., Stos-Gale, Z., Billström, K., Andersen, T., Hannu, H., Albarède, F., 2016. Large-scale tectonic cycles in Europe revealed by distinct Pb isotope provinces. Geochem. Geophys. Geosyst. 17, 3854–3864.
Chen, Y.-Q., Jiang, S.-Y., Ling, H.-F., Yang, J.-H., 2009. Pb–Pb dating of black shales from the Lower Cambrian and Neoproterozoic strata, South China. Chem. Erde 69, 183–189.
DiMarzio, J.M., Georgiev, S.V., Stein, H.J., Hannah, J.L., 2018. Residency of rhenium and osmium in a heavy crude oil. Geochim. Cosmochim. Acta 220, 180–200.
Elder, J.W., 1967. Steady free convection in a porous medium heated from below. J. Fluid Mech. 27, 29–48.
Elshaafi, A., Gudmundsson, A., 2017. Distribution and size of lava shields on the Al Haruj al Aswad and the Al Haruj al Abyad Volcanic Systems, Central Libya. J. Volcanol. Geotherm. Res. 338, 46–62.
England, W.A., Mackenzie, A.S., Mann, D.M., Quigley, T.M., 1987. The movement and entrapment of petroleum fluids in the subsurface. J. Geol. Soc. 144, 327–347.
Evans, D., Graham, C., Armour, A., Bathurst, P. (Eds.), 2003. The Millennium Atlas: Petroleum Geology of the Central and Northern North Sea. Geol. Soc. London.
Fetter, N., Blichert-Toft, J., Télouk, P., Albarède, F., 2019. Extraction of Pb and Zn from crude oil for high-precision isotopic analysis by MC-ICP-MS. Chem. Geol. 511, 112–122.
Finlay, J., Selby, D., Osborne, M.J., Finucane, D., 2010. Fault-charged mantle-fluid contamination of United Kingdom North Sea oils: insights from Re-Os isotopes. Geology 38 (11), 979–982.
Finlay, A.J., Selby, D., Osborne, M.J., 2011. Re-Os geochronology and fingerprinting of United Kingdom Atlantic margin oil: temporal implications for regional petroleum systems. Geology 39, 475–478.
Georgiev, S.V., Stein, H.J., Hannah, J.L., Galimberti, R., Nali, M., Yang, G., Zimmerman, A., 2016. Re–Os dating of maltenes and asphaltenes within single samples of crude oil. Geochim. Cosmochim. Acta 179, 53–75.
Giggenbach, W.F., 1988. Geothermal solute equilibria: derivation of Na-K-Mg-Ca geoindicators. Geochim. Cosmochim. Acta 52, 2749–2765.
Glandt, C.A., Chapman, W.G., 1995. Effect of water dissolution on oil viscosity. SPE Reserv. Eng., 59–64.
Góral, M., Wiśniewska-Gocłowska, B., Mączyński, A., 2004. Recommended liquid–liquid equilibrium data, part 3: alkylbenzene–water systems. J. Phys. Chem. Ref. Data 33, 1159–1188.
Graham, M.D., Steen, P.H., 1994. Plume formation and resonant bifurcations in porous-media convection. J. Fluid Mech. 272, 67–89.
Griswold, J., Kasch, J.E., 1942. Hydrocarbon-water solubilities at elevated temperatures and pressures. Ind. Eng. Chem. 34, 804–806.
Hallett, D., Clark-Lowes, D. (Eds.), 2016. Petroleum Geology of Libya, second edition. Elsevier.
Hunt, J.M., 1984. Generation and migration of light hydrocarbons. Science 226, 1265–1270.
Jiang, S.-Y., Chen, Y.-Q., Ling, H.-F., Yang, J.-H., Feng, H.-Z., Ni, P., 2006. Trace- and rare-earth element geochemistry and Pb–Pb dating of black shales and intercalated Ni–Mo–PGE–Au sulfide ores in Lower Cambrian strata, Yangtze Platform, South China. Miner. Depos. 41, 453–467.
Leventhal, J.S., 1991. Comparison of organic geochemistry and metal enrichment in two black shales: Cambrian Alum Shale of Sweden and Devonian Chattanooga Shale of United States. Miner. Depos. 26, 104–112.
Mackenzie, A.S., Leythaeuser, D., Muller, P., Quigley, T.M., Radke, M., 1988. The movement of hydrocarbons in shales. Nature 331, 63–65.
Mączyński, A., Wiśniewska-Gocłowska, B., Góral, M., 2004. Recommended liquid–liquid equilibrium data, part 1: binary alkane–water systems. J. Phys. Chem. Ref. Data 33, 549–577.
Mahdaoui, F., Michels, R., Reisberg, L., Pujol, M., Poirier, Y., 2015. Behavior of Re and Os during contact between an aqueous solution and oil: consequences for the application of the Re–Os geochronometer to petroleum. Geochim. Cosmochim. Acta 158, 1–21.
Mann, U., 1994. An integrated approach to the study of primary petroleum migration. Geol. Soc. (Lond.) Spec. Publ. 78, 233–260.
Parnell, J., Swainbank, I., 1990. Pb-Pb dating of hydrocarbon migration into a bitumen-bearing ore deposit, North Wales. Geology 18, 1028–1030.
Price, L.C., 1976. Aqueous solubility of petroleum as applied to its origin and primary migration. Am. Assoc. Pet. Geol. Bull. 60, 213–244.
Prinzhofer, A., Girard, J.P., Buschaert, S., Huiban, Y., Noirez, S., 2009. Chemical and isotopic characterization of hydrocarbon gas traces in porewater of very low permeability rocks: the example of the Callovo-Oxfordian argillites of the eastern part of the Paris Basin. Chem. Geol. 260, 269–277.
Selby, D., Creaser, R.A., 2005. Direct radiometric dating of hydrocarbon deposits using Rhenium-Osmium isotopes. Science 308, 1293–1295.
Stacey, J.S., Kramers, J.D., 1975. Approximation of terrestrial lead isotope evolution by a two-stage model. Earth Planet. Sci. Lett. 26, 207–221.
Sverjensky, D.A., 1984. Oil field brines as ore-forming solutions. Econ. Geol. 79, 23–37.
Tissot, B.P., Welte, D.H., 1984. The composition and classification of crude oils and the influence of geological factors. In: Petroleum Formation and Occurrence. Springer, Berlin, Heidelberg.

Ventura, G.T., Gall, L., Siebert, C., Prytulak, Julie, Szatmari, P., Hürlimann, M., Halliday, A.N., 2015. The stable isotope composition of vanadium, nickel, and molybdenum in crude oils. Appl. Geochem. 59, 104–117.
Walters, C.C., 2017. Origin of petroleum. In: Hsu, C.S., Robinson, P.R. (Eds.), Springer Handbook of Petroleum Technology. Springer, Cham. Part B, Chap. 10.
Zanella, E., Coward, M.P., 2003. Structural framework. In: Evans, D., Graham, C., Armour, A., Bathurst, P. (Eds.), The Millennium Atlas: Petroleum Geology of the Central and Northern North Sea. Geol. Soc. London. Chap. 4.
Ziegler, P.A., 1992. North Sea rift system. Tectonophysics 208, 55–75.